Far-infrared optical transitions in a corrugated interface under normally applied electric fields

1995 J. Phys.: Condens. Matter 7 6483

(http://iopscience.iop.org/0953-8984/7/32/014)

J. Phys.: Condens. Matter 7 (1995) 6483–6491. Printed in the UK

Far-infrared optical transitions in a corrugated interface under normally applied electric fields

Zhen-Yan Deng†‡, Yu-Feng Zhang‡ and Jing-Kun Guo‡

† China Centre of Advanced Science and Technology (World Laboratory), PO Box 8730, Beijing 100080, People's Republic of China

‡ The State Key Laboratory of High Performance Ceramics and Superfine Microstructure, Shanghai Institute of Ceramics, Chinese Academy of Sciences, Shanghai 200050, People's Republic of China

Received 14 February 1995, in final form 25 April 1995

Abstract. We calculate the subband structures and inter-subband transitions in a corrugated GaAs–AlAs interface under normally applied electric fields. It is found that the first energy minigap of the system can be tuned linearly using the normally applied electric fields, and an anisotropy in the inter-subband optical absorptions exists for a linearly polarized incident light wave. The dependence of the inter-subband transition spectra on the interface structures and external electric fields is discussed.

1. Introduction

With advances in the art of microfabrication, it has become possible to confine carriers in one, two or all three dimensions. Recently, a new quantum well structure emerged, in which there are periodic lateral surface structures on its interfaces which act as periodic potentials on electrons. This novel system, referred to as a lateral surface superlattice (LSSL), has shown interesting electronic and optical properties [1–5]. Of the various LSSL structures, the GaAs/AlAs LSSL seems to offer the greatest potential for wide applications in microelectronics and electro-optics [2, 3], due to the large band offsets between GaAs and AlAs which enhance the effects of interface structures on the motion of electrons. In fact, electronic wave interference devices using GaAs/AlAs LSSLs have been designed by Fukui *et al* [6] and a variety of peculiar electronic properties in the LSSLs have been predicted by several researchers theoretically [7–11].

By a coordinate transformation which transforms periodically structured interfaces into planar interfaces so that the continuity of electron wavefunctions can be satisfied exactly on the interfaces, Sun [8, 9] has studied subband structures and their optical absorptions in GaAs/AlAs LSSLs intensively. Their results are interesting. Technically, it is easier to fabricate an interface with periodic lateral surface structures, referred to as an interface lateral superlattice (ILSL), than the LSSL [12]. In this paper, we study the inter-subband transitions in a GaAs/AlAs ILSL under normally applied electric fields. Because the electric fields push the electrons towards the interface, the effects of interface structures on the motion of electrons become important. It is expected that the peculiar electronic properties in LSSLs could appear in ILSLs. In section 2, we outline the theory framework. The results and discussion are presented in section 3.

0953-8984/95/326483+09$19.50

2. Theory

In the effective-mass approximation, the Hamiltonian of the GaAs/AlAs ILSL can be written

$$H(r) = \frac{|P|^2}{2m} + V(r) + eFz \tag{1}$$

where P and r are the electron momentum and coordinate, respectively; $m = 0.067m_0$ is the electron-band effective mass in GaAs with m_0 the free-electron mass, and F is the external electric-field strength applied normally to the interface. For simplicity, the potential barrier between the GaAs and AlAs is assumed to be infinite:

$$V(r) = \begin{cases} 0 & z > f(r) \\ \infty & \text{elsewhere} \end{cases} \tag{2}$$

where $f(r)$ describes the periodic lateral structures on the GaAs–AlAs interface.

As in [8, 9], the following coordinate transformation is introduced which transforms the structured interfaces into flat interfaces:

$$\begin{aligned} x' &= x \\ y' &= y \\ z' &= z - f(r). \end{aligned} \tag{3}$$

In the transformation, we note that

$$\int_V \psi^*(r)H(r)\psi(r)\,\mathrm{d}\tau = \int_{V'} \tilde{\psi}^*(r')J(r')\tilde{H}(r')\tilde{\psi}(r')\,\mathrm{d}\tau' = \int_{V'} \tilde{\psi}^*(r')H_{\text{eff}}(r')\tilde{\psi}(r')\,\mathrm{d}\tau' \tag{4}$$

where $J(r')$ is the Jacobian determinant, and the effective Hamiltonian is defined as

$$H_{\text{eff}}(r') = J(r')\tilde{H}(r'). \tag{5}$$

The normalization condition becomes

$$\int_{V'} \tilde{\psi}^*(r')\tilde{\psi}(r')J(r')\,\mathrm{d}\tau' = 1. \tag{6}$$

After the coordinate transformation, the electron-confining potential well $\tilde{V}(r')$ is

$$\tilde{V}(r') = \begin{cases} 0 & z' > 0 \\ \infty & \text{elsewhere.} \end{cases} \tag{7}$$

In the new coordinate system, the wavefunction satisfies the boundary condition

$$\tilde{\psi}(r')|_{z'=0 \text{ or } \infty} = 0. \tag{8}$$

For a model calculation, the periodic interface structures are assumed to be

$$f(r) = \Delta \sin\left(\frac{2\pi}{L_x}x\right) \tag{9}$$

where Δ and L_x are the amplitude and period, respectively, of the interface structures.

Because of the existence of the externally applied electric fields, the electron-confining potential in the z direction in the new coordinate space is a triangular potential, as shown in figure 1(a). The ground wavefunction of the ILSL in the z direction is an Airy function [13], which can be expressed by the Bessel function with $-1/3$ fractional order:

$$\varphi_0(z') = N_0 \xi^{1/2} J_{-1/3}(\tfrac{2}{3} i \xi^{3/2}) \tag{10}$$

where N_0 is the normalization constant and

$$\xi = \left(\frac{m}{\hbar^2}\right)^{1/3} \left((2eF)^{1/3} z' - \frac{2E_z^{(1)}}{(2eF)^{2/3}}\right) \tag{11}$$

with $E_z^{(1)}$ the ground level in the z direction, which is determined by the first zero $x_1 = 1.8597$ of the Bessel function $J_{-1/3}(x)$:

$$E_z^{(1)} = \frac{1}{2}\left(\frac{\hbar^2}{m}\right)^{1/3} (3eFx_1)^{2/3}. \tag{12}$$

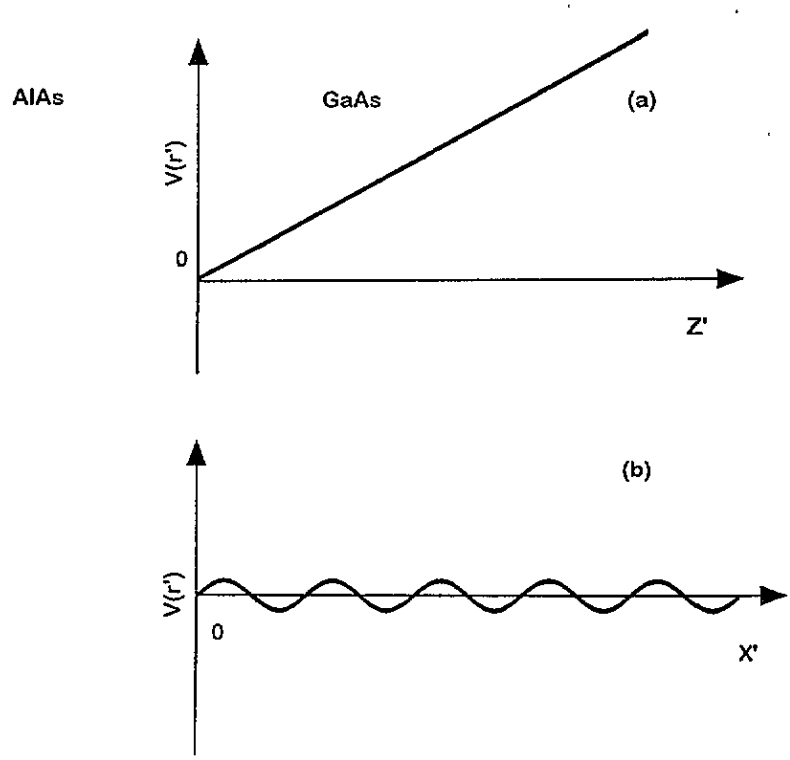

Figure 1. Schematic representation of the electron-confining potential in the GaAs/AlAs ILSLs in the new coordinate space: (a) the triangular potential in the z direction; (b) the periodic potential with lateral period L_x in the x direction.

The periodic lateral structures on the interfaces act as a periodic potential in the new coordinate system, as shown in figure 1(b), which causes reflections of the electron plane waves in the x direction. Energy minigaps (EMGs) appear in the electronic energy dispersions at the boundaries of the Brillouin zones in the x direction. Now, we calculate the subband dispersions of the ILSLs with the variational approach.

$$E = \left(\int_V \psi^*(r)H(r)\psi(r)\,d\tau\right)\Big/\left(\int_V \psi^*(r)\psi(r)\,d\tau\right)$$
$$= \left(\int_{V'} \tilde{\psi}^*(r')H_{\text{eff}}(r')\tilde{\psi}(r')\,d\tau'\right)\Big/\left(\int_{V'} \tilde{\psi}^*(r')\tilde{\psi}(r')J(r')\,d\tau'\right) \tag{13}$$

where $\tilde{\psi}(r')$ represents the variational wavefunction in the new coordinate spaces.

Because we are interested in the behaviours of electrons at the boundaries of Brillouin zones, the two-wave approximation approach for calculating the first and second subband dispersions is reasonable [14].

$$\tilde{\psi}_k(r') = A\varphi_k^{(1)}(r') + B\varphi_k^{(2)}(r') \tag{14}$$

with

$$\varphi_k^{(1)}(r') = \varphi_0(z')\exp(ik_x x' + ik_y y') \tag{15}$$

and

$$\varphi_k^{(2)}(r') = \varphi_0(z')\exp[i(k_x - k_d)x' + ik_y y'] \tag{16}$$

where A and B are the variational parameters, and $k_d = 2\pi/L_x$ is the first reciprocal-lattice vector in the x direction. Inserting the trial wavefunction (14) and the effective Hamiltonian (5) into equation (13), we can obtain the first and second electronic subband dispersions by minimizing E (equation (13)) with respect to A and B, which give the following equation:

$$\det \| H_{\text{eff}}^{(ij)}(k) - E_{1,2}(k)J^{(ij)}(k)\| = 0 \qquad (i, j = 1, 2) \tag{17}$$

with the matrix elements

$$H_{\text{eff}}^{(ij)}(k) = (\varphi_k^{(i)}(r')|H_{\text{eff}}(r')|\varphi_k^{(j)}(r')) \tag{18}$$

and

$$J^{(ij)}(k) = (\varphi_k^{(i)}(r')|J(r')|\varphi_k^{(j)}(r')). \tag{19}$$

The first EMG at the boundary of Brillouin zone in the x direction is obtained as

$$\Delta E_g(1) = eF\Delta. \tag{20}$$

which indicates that the first EMG can be tuned linearly by adjusting the external electric-field strength and the amplitude of interface structures and is independent of the interface lateral period.

In the dipole approximation, the inter-subband optical absorption coefficient for a linearly polarized plane electromagnetic wave in an ILSL with a refractive index n is given by [9–11]

$$W(\omega) = \frac{\pi e^2}{nc\epsilon_0 m^2 V\omega} \sum_{ifk} |\varepsilon \cdot \boldsymbol{P}_{if}(k)|^2 \delta[(E_f(k) - E_i(k) - \hbar\omega] \tag{21}$$

where ϵ_0, V and $\hbar\omega$ represent the permittivity of free space, the sample volume and the photon energy, respectively. ε is the polarized vector defining the orientation of the electric field of the linearly polarized wave. It is assumed that any initial electronic state i is occupied and any final electronic state f is unoccupied. The optical transition vector $\boldsymbol{P}_{if}(k)$ between the initial and final states is defined by [9]

$$\begin{aligned} \boldsymbol{P}_{if}(k) &= \int_V [u_f(r)\psi_{fk}(r)]\boldsymbol{p}[u_i(r)\psi_{ik}(r)]\,\mathrm{d}\tau \\ &= \int_V \psi^*_{fk}(r)\psi_{ik}(r)\,\mathrm{d}\tau \int_\Omega u^*_f(r)\boldsymbol{p}u_i(r)\,\mathrm{d}\tau/\Omega \\ &\quad + \int_V \psi^*_{fk}(r)\boldsymbol{p}\psi_{ik}(r)\,\mathrm{d}\tau \int_\Omega u^*_f(r)u_i(r)\,\mathrm{d}\tau/\Omega \end{aligned} \tag{22}$$

where Ω is the primitive unit-cell volume of the GaAs crystal; $u_{i,f}(r)$ is the electron Bloch function at the bottom of conduction band; $\psi_{i,fk}(r)$ are the envelope functions of the initial and final states, i.e. the first and second conduction subbands, respectively. The first term of equation (22) is zero due to the orthogonal relation between the wavefunctions of the first and second conduction subbands. In the new coordinate system, we obtain that the only nonzero optical transition matrix is the x component of $\boldsymbol{P}_{if}(k)$, which is given by

$$P_x(k) = \int_{V'} \tilde{\psi}^*_{2k}(r')\frac{\hbar}{\mathrm{i}}\left(\frac{\partial}{\partial x'} - \frac{\mathrm{d}f(x')}{\mathrm{d}x'}\frac{\partial}{\partial z'}\right)\tilde{\psi}_{1k}(r')\,\mathrm{d}\tau'. \tag{23}$$

Then

$$|\varepsilon \cdot \boldsymbol{P}_{if}(k)|^2 = |P_x(k)|^2 \cos^2\theta \tag{24}$$

where θ is the angle between the polarized vector of the linearly polarized incident light wave and the x direction.

The disorder fluctuation of the interface structures of the ILSL from the ideal periodic structures (9) is taken into consideration by introducing a distribution of the amplitude Δ in the interface structures, which for model calculation is taken to be

$$P(\Delta) = \begin{cases} P_0 \exp[-(\Delta - \Delta^{(0)})^2/2] & \text{for } \Delta > 0 \\ 0 & \text{otherwise} \end{cases} \tag{25}$$

where Δ is in ångströms and P_0 is determined by

$$\int P(\Delta)\,\mathrm{d}\Delta = 1. \tag{26}$$

The averaged optical absorption coefficient is given by

$$\overline{W(\omega)} = \int P(\Delta)W(\omega, \Delta)\,\mathrm{d}\Delta. \tag{27}$$

3. Discussion

Figure 2 shows the first two conduction subband energy dispersions in the GaAs/AlAs ILSL for different external electric fields. From figure 2, we can see that EMGs appear in the electronic energy dispersions at the boundaries of the Brillouin zones in the x direction, and the EMG increases with increase in the external electric-field strength. From figure 2 and equation (20), we can also see that the first conduction EMG in the GaAs/AlAs ILSLs can be tuned from zero to tens of millielectronvolts by adjusting the amplitude of the interface structures and the external electric field, which can be obtained experimentally [1–3, 13].

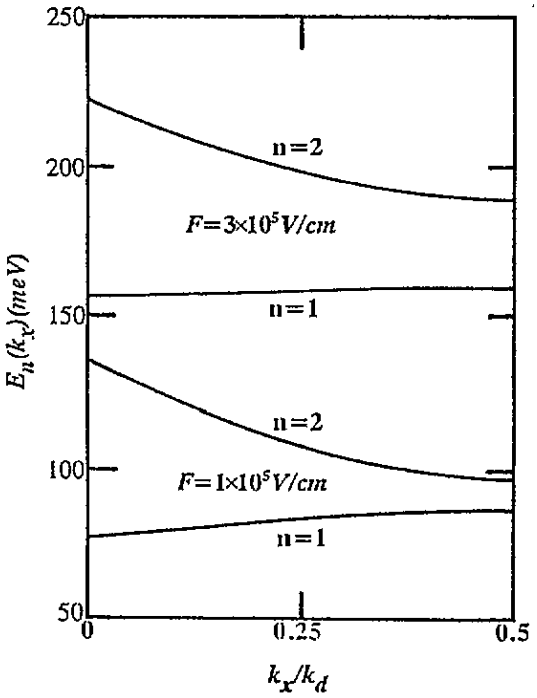

Figure 2. The electronic energy dispersions of the first two conduction subbands $E_n(k_x) = E_n(k) - \hbar^2 k_y^2/2m$ in the GaAs/AlAs ILSL for different external electric-field strengths, where the structural parameters are $L_x = 200$ Å and $\Delta^{(0)} = 10$ Å, and the disorder fluctuation of interface structures is not considered.

Figure 3 shows the averaged optical absorption coefficient as a function of the photon energy $\hbar\omega$ for different electric-field strengths and disorder fluctuations. In figure 3, it is apparent that the energy-forbidden region exists for the optical transitions from the first conduction subband to the second conduction subband; the width of the energy-forbidden region and the position of the optical absorption peak increase with increase in the electric-field strength. In figure 3, we can see that, when a disorder fluctuation of the interface structures in the GaAs/AlAs ILSL exists, firstly the energy-forbidden region decreases, secondly the width of the optical absorption spectra increases and thirdly the position of the optical absorption peak shifts slightly to a high energy, compared with those in

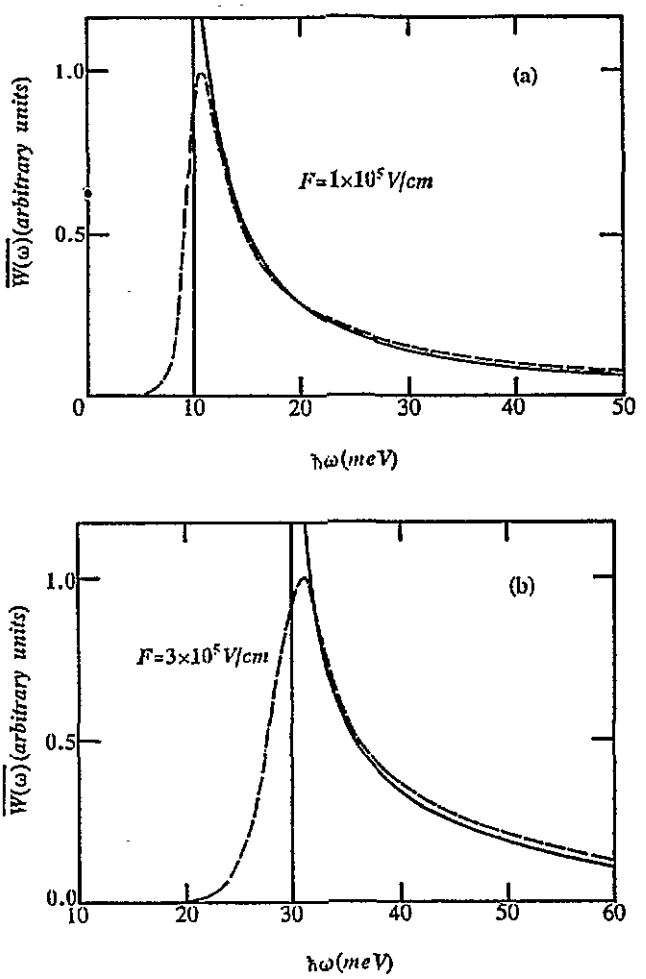

Figure 3. The averaged optical absorption coefficient as a function of the photon energy $\hbar\omega$ for different electric-field strengths (a) $F = 1 \times 10^5$ V cm^{-1} and (b) $F = 3 \times 10^5$ V cm^{-1}, where the structural parameters of the GaAs/AlAs ILSLs are $L_x = 200$ Å and $\Delta^{(0)} = 10$ Å. The solid and broken curves represent the optical absorption coefficient excluding and including the disorder fluctuation of interface structures, respectively.

the GaAs/AlAs ILSL without disorder fluctuation. Also, the larger the external electric-field strength, the wider the optical absorption spectra is, when the disorder fluctuation is considered.

Figure 4 shows the dependence of the relative intensity of optical absorption spectra on the polarized angle θ of the incident light wave in the GaAs/AlAs ILSLs. From figure 4, we can see that the intensity of optical absorption spectra decreases with increase in the polarized angle θ. When the polarized angle $\theta = 0°$, i.e. the polarized vector of the incident light wave is parallel to the direction of the interface structures, the intensity of the optical absorption spectra is a maximum. When the polarized angle $\theta = 90°$, i.e. the polarized vector of the incident light wave is normal to the direction of the interface structures, the intensity of optical absorption spectra is zero. These indicate that the inter-subband absorption spectra in the GaAs/AlAs ILSLs are anisotropic for different orientations of the

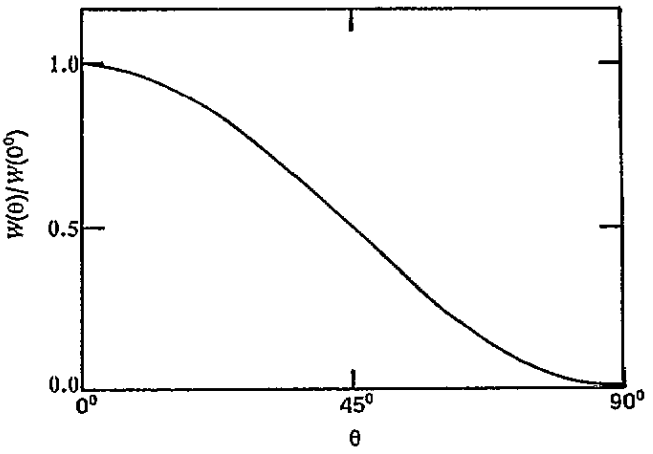

Figure 4. The relative averaged optical absorption coefficient of the GaAs/AlAs ILSLs as a function of the polarized angle θ of the incident light wave.

polarized vector of the incident light wave.

The results obtained above are interesting and the physical interpretations are as follows. Because of the existence of the external electric field which is normally applied to the interface, the electrons shift towards the interface and the effects of the interface structures on the motion of electrons become important. The interface periodic lateral structures act as periodic potentials which cause reflections of the electron plane waves in the x direction, and EMGs appear in the electronic energy dispersions at the boundaries of the Brillouin zones in the x direction; so there is an energy-forbidden region in the inter-subband optical absorption of GaAs/AlAs ILSLs. When the external electric-field strength increases, the confinement of the electrons in the vicinity of the interface strengthens and the effects of the interface structures on the motion of electrons are enhanced. These result in increases in the first conduction EMG and the energy-forbidden region of the optical absorption spectra in the GaAs/AlAs ILSLs. When a disorder fluctuation of the interface structures exists, a corresponding fluctuation in the first conduction EMG appears, which can be seen from equation (20). This is the reason why the width of the optical absorption spectra increases and the energy-forbidden region of the optical absorption spectra decreases. In addition, the anisotropy of the inter-subband optical absorptions in the GaAs/AlAs ILSLs arises because the interface lateral structures exist only in the x direction and the effects of interface structures are important only for electrons moving in the x direction [2, 3].

In the above calculation of the inter-subband optical absorption spectra, we have neglected the effect of electron–electron interactions. By a method similar to that used in [9], we have estimated the effects of electron–electron interactions on the first conduction EMG. The results indicated that the change in the first conduction EMG is within 35%, and the main characteristic of the inter-subband optical absorptions in the GaAs/AlAs ILSLs that we considered can be described by a noninteraction electron model.

Summing up, we have studied the subband structures and the inter-subband optical absorptions in the GaAs/AlAs ILSLs. The results showed that the first conduction EMG in the GaAs/AlAs ILSL can be tuned linearly by the normally applied electric fields, and an energy-forbidden region exists for the optical transitions from the first conduction subband to the second conduction subband. The results also showed that anisotropy exists for the inter-subband optical absorptions when the orientation of the polarized vector of the incident light

wave varies with respect to the interface structure direction. We hope that our theoretical results stimulate further experimental investigations.

References

[1] Tanaka M and Sakaki H 1988 *Japan. J. Appl. Phys.* **27** L2025
[2] Tsuchiya M, Gaines J M, Yan R H, Simes R J, Holtz P O, Coldren L A and Petroff P M 1989 *Phys. Rev. Lett.* **62** 466
[3] Tanaka M and Sakaki H 1989 *Appl. Phys. Lett.* **54** 1326
[4] Gerhardts R R, Weiss D and von Klitzing K 1989 *Phys. Rev. Lett.* **62** 1173
[5] Winkler R W and Kotthaus J P 1989 *Phys. Rev. Lett.* **62** 1177
[6] Fukui T, Tsubaki K, Saito H, Kasu M and Honda T 1992 *Surf. Sci.* **267** 588
[7] Citrin D S and Chang Y C 1991 *J. Appl. Phys.* **70** 867
[8] Sun H 1992 *Phys. Rev.* B **46** 12371
[9] Sun H 1993 *Phys. Rev.* B **48** 17906
[10] Bockelmann U and Bastard G 1992 *Phys. Rev.* B **45** 1688
[11] Bockelmann U and Bastard G 1992 *Phys. Rev.* B **45** 1700
[12] Sham L J 1991 *Proc. Int. Semin. on Physics of Semiconductor Interfaces and Heterostructures (Beijing, 1991)*
[13] Austin E J and Jaros M 1985 *Phys. Rev.* B **31** 5569
[14] Deng Z Y, Lai T R, Guo J K, Sun H and Gu S W 1994 *J. Phys.: Condens. Matter* **6** 5681